Egyptian Geophysical Society
EGS Journal, Vol. 15, No. 1, 185-198 (2017)

APPLICATIONS OF SHALLOW SEISMIC REFRACTION AND SURFACE WAVES (MASW) FOR INFERRINGTHE GEOTECHNICAL CHARACTERISTICS AT CAIRO-BILBEIS AREA, EAST NILE DELTA REGION, EGYPT

A.M. El-Rawy[(1)], M.I. Mohamed[(2)] and A.S. Helaly[(1)]

(1) Department of Geophysics, Faculty of Science, Ain Shams University, Cairo, Egypt.
(2) Helal Group for Geotechnical-Geological-Geophysical Services, Cairo, Egypt.

تطبيقات الموجات السيزمية الانكسارية والموجات السطحية (ماسو) لاستنتاج الخصائص الجيوتقنية بمنطقة القاهرة - بلبيس ، شرق دلتا النيل، مصر

الخلاصـــة: تقع منطقة الدراسة داخل نطاق القاهرة-بلبيس ، شرق دلتا النيل ، مصر . كان الهدف الرئيسى من اجراء الدراسة هو استخدام تقنيـــات الموجات السيزمية الانكسارية المقطعية وكذلكتحليل بيانات الموجات السطحية لمعرفه توزيعات السرعات تحديد المعاملات الجيوتقنية والخواص الهندسية لمنطقة الدراسة. وقد تم جمع البيانات السيزمية من خلال خمس خطوط سيزمية انكسارية مقطعية لحساب سرعة الموجات التضاغطية وسرعة الموجات المستعرضة وذلك لعمل نموذج للطبقات السطحية والتحت سطحية لمنطقة الدراسة.تم قياس ستة عشر بروفيل للموجات السيزمية الانكسارية الضحلة وذلك من خلال سبع ضربات موزعة خلال كل بروفيل. اجماليا تم قياس ١١٢ سجل خلال الخمس خطوط. حيث أن الخط السيزمى الأول يتكون من أربعـــة بروفيلات أما الخطوط الآخري تتكون من ثلاثة بروفيلات.وقد خضعت هذه القياسات لبعض التصحيحات ثم إنشاء قطاعات للموجة الانضغاطية و الموجات المستعرضة باستخدام طريقة التصوير المقطعي السيزمى وطريقة النمذجة العكسية وذلك لتحسين نماذج السرعات المستنبطة للطبقات التحت سطحية .بعد ذلك تم حساب عدد من المعاملات الجيوتقنية والخصائص الديناميكية مثل الكثافة ، نسبة بواسون، معامل يونج، معامل الصلابة ، معامل الحجم ، فئة الموقع، مؤشر المواد، مؤشر التركيز ، نسبة الإجهاد ، وقدرة التحمل لتقييم طبقات التربة السطحية والقريبة من السطح باستخدام السرعات السيزمية (الانضغاطية والمستعرضة).و من خلال هذه الدراسة تم التعرف على عدد الطبقات الموجودة و كذلك معلومات عن هذه طبقات التربة مثل نوعية التربة . وقد تبين أن قطاع التربة في منطقة الدراسة يتكون من ثلاث طبقات فوق الطبقات الصخرية. صنفت طبقات التربة التحت سطحية الضحلة لمنطقة الدراسة إلى فئتين (جـــ ، د) وفقا لنظام تصنيف الموقع نيرب لسنة (٢٠٠٣).

ABSTRACT: *Shallow Seismic Refraction Tomography and Multichannel Analysis of Surface Waves (MASW) field methods were conducted at an area located within Cairo-Bilbeis area, East Nile Delta Region, Egypt. The aim of the study is the use of these techniques for determining the geotechnical parameters and engineering site characteristics of the area under investigation. The seismic data were collected along five seismic lines to estimate the compressional (V_p) wave velocity and shear (V_s) wave velocity for delineating the near-surface ground model beneath the study area. Sixteen shallow seismic refraction spreads were carried out, each through seven shots located within each spread. Totally 112 shot records have been acquired through the five lines, the first seismic line consists of four spreads and the others consist of three spreads. Compressional and shear wave spreads were created, using the seismic refraction method and data inversion has been made to minimize the error between the observed and calculated travel times and to improve the velocity models. A number of geotechnical parameters and dynamic characteristics; such as Density, Poisson's Ratio, Young's Modulus, Rigidity Modulus, Bulk Modulus, Site Class, Material Index, Concentration Index, Stress Ratio and Ultimate Bearing Capacity (Q_{ult}) were calculated to assess the near-surface soil competency from the seismic velocities (compressional and shear). Soil layers quality is interpreted, using the obtained velocity types. The soil sections within the study area consist of three layers above the bedrock. The near-surface soil layers evaluatedin the study area were classified into two site classes, (D and C), according to the Site Classification Scheme of NEHRP Provisions (2003)*

INTRODUCTION

Conventional near-surface geotechnical site investigations are often made by mechanical techniques (e.g. boreholes, Standard Penetration Test (SPT), Cone Penetration Test (CPT), Flat Plate Dilatometer Test (DMT), Dynamic Cone Penetrometer (DCP), and density tests, among others). These well-known classical techniques are widely accepted as reliable methods, within the geotechnical community. However, information recovered by these techniques are localized to the point, at which the test is conducted. Therefore, an adequate number of seismic tests must be conducted at distributed points throughout the site, in order to make fair assessment for the soil, rendering the investigation both costly and protracted for an extensive site (Tokeshi et al., 2013).

Elastic properties of the near-surface materials and their effects on the seismic wave propagation are of fundamental interest in groundwater, engineering, and environmental studies. Shear wave (V_s) velocity is a key parameter in the construction engineering. The use of surface waves for the estimation of shear wave velocity profiles has received considerable attention over the last number of years. The Multichannel Analysis of Surface Waves (MASW) method is one of the more recently

developed techniques. It makes use of the multichannel recording techniques, that have similarities to those used in the CMP body wave reflection surveys. The MASW method was first introduced in the late 1990's by Park et al. (1997) and Xia et al. (1999). The MASW method is concerned with the shallow depths (e.g. less than 30 m), that are of interest to civil engineers.

The study area lies at the northeastern part of Greater Cairo (Egypt) within the eastern part of the Nile Delta. It is located between latitudes 30°15'31.00" & 30°16'52.00"N and longitudes 31°26'10.00" & 31°28'50.00"E (Figure 1).Sixteen shallow seismic refraction tomography profiles were carried out in the study area. The collected data were used to estimate the compressional wave and shear wave velocities for delineating the near-surface ground model and to study the geotechnical characteristics of the study soil.

Geologic Setting

The surface geology and stratigraphic description of the study area were studied in detail by the Geological Survey of Egypt and Mining Authority (EGSMA, 1998)through the fieldwork trips and Inshas borehole drilled (Figure 2) at the western part of the study area. Most parts of the geological units in the study area belong to the Quaternary and Middle Miocene periods.

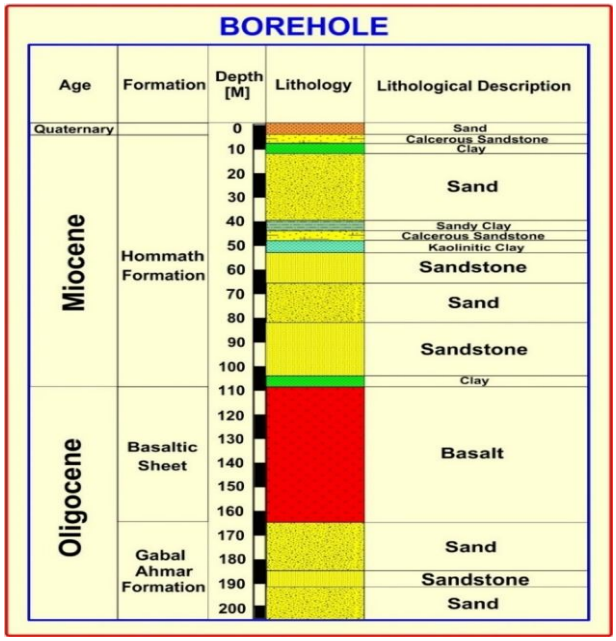

Figure (2): Lithologic log from the borehole drilled by EGSMA (1998).

The Quaternary (Holocene and Pleistocene) deposits are represented by sand sheet cover at the western part of the study area. These clastic deposits are represented by two formations; the first one is *Inshas Formation,* which consists of cross-bedded sand intercalated with nile mud and silt. The second formation is *Bilbies Formation,* which consists of medium-to coarse-grained sand with plant roots, intercalated with flint, chert and clay, which cover most part of the study area. The Tertiary deposits are represented by *Hommath Formation* which consists of sandy limestone, sandstone and sandy marl of Middle Miocene age, and covers the southeastern part of the study area (Figure 3). The Oligocene deposits are represented by *Gabal Ahmer Formation*, which is composed of sand and sandstone, according to EGSMA (1998).

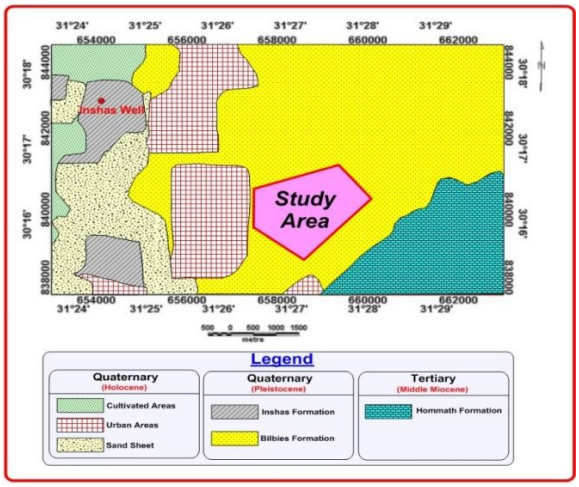

Figure (3): Geological map of the study area (after EGSMA 1998).

The subsurface section within the study area is characterized by low seismic activity. However, a number of moderateto large size earthquakes occurred in the Mediterranean and Red Seas, as well as the Gulf of Suez and Gulf of Aqaba, which affected the area with intermediate earthquake intensity (e.g., seismic hazard <100 cm/ S^2) (Riad et al., 2000). In a more recent study, the seismic hazard map developed by El-Hadidy (2012) demonstrates that, the seismic hazard around the study area is 75–100 cm/S^2, as shown in Figure (4).

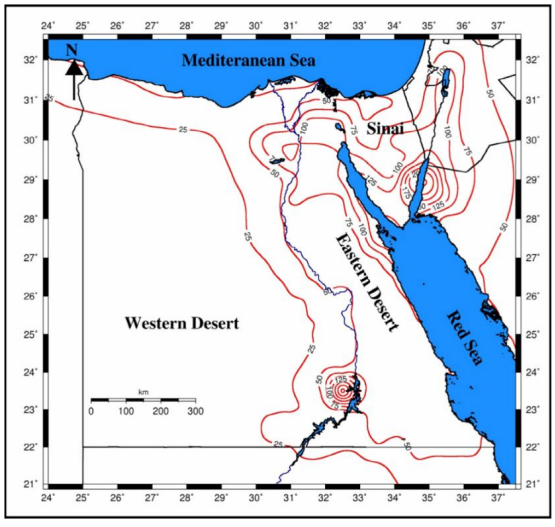

Figure (4): Mean peak ground acceleration (cm/S^2) with 10% probability of exceedance in 50 years (475 years return period) in Egypt (after El-Hadidy, 2012).

Multichannel Analysis of Surface Waves (MASW) Technique

The Multichannel Analysis of Surface Waves (MASW) technique (Park et al., 1997&1999) involves a source; such as a sledgehammer impact on the ground (Figure 5). Vibrations generated due to the sledgehammer impact are gathered by interconnected electromagnetic geophones (receivers) set up in the vertical direction and in a linear array, with a constant spacing at the ground surface, to obtain the experimental Rayleigh wave phase velocity dispersion curve. Usually several shots of the sledgehammer are performed at both extremes of the array to ensure that, reliable and clear dispersion curves are obtained (Tokeshi et al., 2013).

MASW method utilized the phase velocity of surface waves (Rayleigh waves or ground rolls), that are typically considered as noises for seismic surveys to estimate the shear wave velocity (V_s) profiles (Park et al., 1998). Rayleigh wave phase velocity is a function of the frequency and subsurface properties including V_p, V_s, density and layer thickness. In a homogeneous medium, the Rayleigh wave has phase velocity ranges from 0.87 to 0.96 of V_s (Richart et al., 1970) over a range of Poisson's ratio, whereas it has dispersion characteristics in a vertically heterogeneous medium. MASW data were recorded by the same manner, as the conventional seismic reflection/refraction acquisition (Figure 5) (Yordkayhun et al., 2014).A multiple number of receivers (usually 24 or more) are deployed with even spacing along a linear survey line, with receivers connected to a multichannel recording device (seismograph) (Figure 5). Each channel is dedicated to record the vibrations from one receiver.

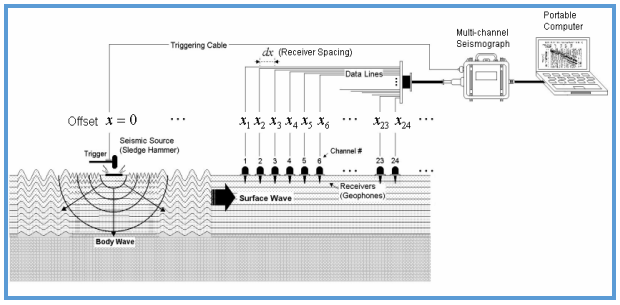

Figure (5): A schematic of a typical MASW survey configuration (after Park et al., 2005).

The generated seismic waves in all seismic surveys have the strongest energy (more than two-thirds of the total energy are carried by the ground roll) and hence the Rayleigh waves appear as dominant events in the seismic records. Their vertical propagation in a vertically heterogeneous (i.e. layered) medium exhibits a dispersive behavior. The term dispersion implies that, different frequencies have different phase velocities. Unlike in a homogeneous medium, where all wavelengths have the same velocity on account of the same material everywhere, while in heterogeneous medii the surface waves exhibit differences in their behaviors. There occurs an exponential decrease in their amplitude with depth and most of the energy propagates in a shallow zone (roughly the length of one wavelength). In a layered medii, the surface waves do not have a single velocity, but a phase velocity that is a function of the frequency. This relation between the frequency and the phase velocity is known as the dispersion curve. At higher frequency values, the phase velocity is the Rayleigh velocity of the uppermost layer of the medium; whereas at lower frequency values, the effect of deeper layers becomes more and more dominant with the result that, the phase velocity tends asymptotically to Rayleigh velocity of the material in the deepest layer. This dispersive nature of the Rayleigh waves is utilized in the MASW technique to map the values of shear wave velocities (V_s) in the subsurface (Kesarwani et al., 2012).

Data processing involves three steps (Figure 6): 1) preliminary detection of the surface waves, 2) constructing the dispersion image panel and extracting the signal dispersion curve, and 3) back-calculating the shear wave velocity (V_s) variation with depth. All these steps can be fully automated. The preliminary detection of surface waves examines the recorded seismic waves in the most probable range of frequencies and phase velocities. Construction of the image panel is accomplished through a 2-D (time and space) wave field transformation method that employs several pattern-recognition approaches (Park et al., 1998b).

Seismic Refraction Tomography Technique:

The seismic refraction technique involves the estimation of the acoustic P-wave velocity within the earth's near-surface soils to depths typically less than100feet. The fundamental principle behind seismic refraction technique is the measurement of travel times of the seismic waves refracted at the interfaces between the subsurface layers of different velocities. The seismic energy generated by a seismic source ('shot') located on the surface radiates seismic waves from the shot point, which spread in all directions. They may either travel directly through the upper layer (direct arrivals), or they may travel down through the layer and then laterally along the boundaries with the high velocity layers before bouncing up and coming back to the surface (refracted arrivals). The gained seismic data are recorded by a seismograph and the travel times versus distances curves are then displayed. These curves are utilized to calculate the velocities of the overburden and refracting layers. Considering the shot and receiver geometry, the analysis of the measured travel-times and the calculated velocities gives the depth profiles for each refractor.

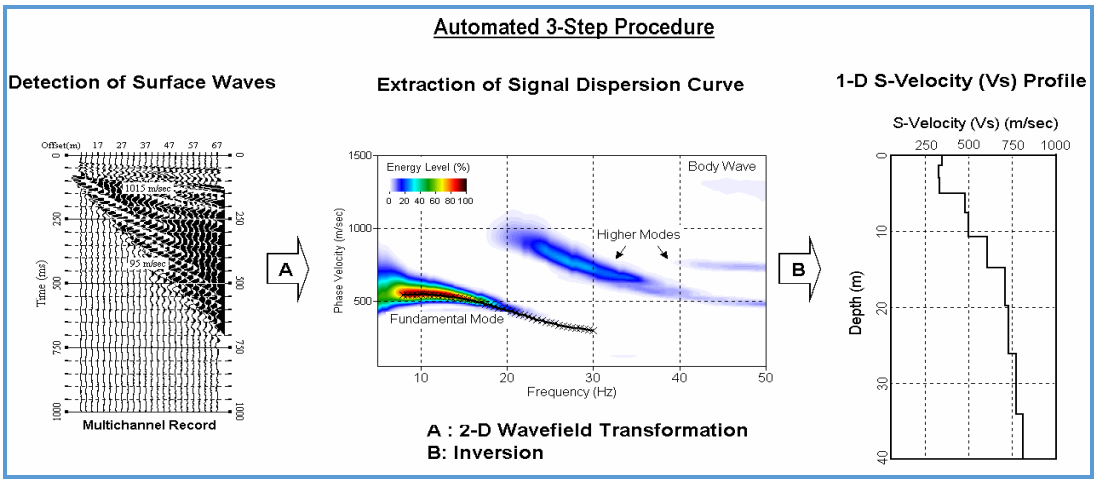

Figure (6): A 3-step scheme for MASW data processing illustrated by an actual field data set (after Park et al., 2005).

The final output hence comprises the depth profile of the refracting layers and the velocity model of the subsurface. The primary applications of the seismic refraction technique are for determining the depths to bedrock and bedrock structure. Because of the dependence of seismic velocitieson the elasticity and density of the materials composing of the subsurface layers through which they are passing, seismic refraction surveys also give a measure of material strengths. Consequently they act as an aid in assessing rock strength and rock quality (Kesarwani et al., 2012).

Field Measurements:

The study area covers an area of approximately 1.6 square kilometers within the Cairo-Bilbeisarea, East Nile Delta. Five survey lines of seismic refraction consist of 16 Seismic Refraction profiles are performed at the study area.

Each seismic refraction profile acquired with seven shots located through each profile. Totally 112-shot records have been recorded through the five lines, the first seismic line consists of four spreads and the others consist of three spreads. The seismic refraction data were collected using the OYO McSeisSX24 channel Seismograph. The first line (Line 1) consists of 4 seismic spreads with a length of about 800 m and the other 4 lines (Line 2, Line 3, Line 4 and Line 5) consist of 3 seismic spreads with a length of 612.5 m, as shown in the shot-point location map (Figure 7). Each seismic refraction spread (Figure 8) has 24 receivers with interval of 7.5 m and sevens hot points located as **follows**:

1) Offset Normal [ON]: located at an offset distance of 57.5 meter before the first geophone.
2) Normal [N]: located at an offset distance of 7.5 meter before the first geophone.
3) Normal-Middle [NM]: located at the middle point between geophones no. 6&7.
4) Middle [M]: located at the middle point between geophones no. 12&13.
5) Reverse-Middle [RM]: located at the middle point between geophones no. 18&19.
6) Reverse [R]: located at an offset distance of 7.5 meter after the last geophone.
7) Offset Reverse [OR]: located at an offset distance of 57.5 meter after the last geophone.

The sledgehammer was used as the seismic source. To reduce noises, and improve the data quality in each shot, the sum of common shot records was used and recorded as the stacked record. The number of stacks per shot point ranged between 5 and 10, depending on the quality of recorded signals. The number of geophones is twenty four, while the data set comprises 2,688 traces. To determine the accurate velocity for each layer using the refracted waves, the accurate determination of the first-break arrival times is required.

Data Analysis and Interpretation

The collected 116 shot records were subjected to some processes; such as sorting, editing and applying some filters to increase the signal to noise ratio, using the Geogiga Seismic Pro. 7.1 software. The first step in the processing sequence was the data sorting for each seismic line, then editing the acquired data through defining the locations of shot points and receivers along each seismic spread.

Filters were applied to the shot records; such as high pass and low pass filters. High-pass filter is used to remove the low frequency noises of less than 1 Hz, while the low-pass filter is used to remove the high frequency noises of more than 100Hz. Shot records were transformed by the Fourier transform function to the amplitude spectrum, in order to apply the filters.

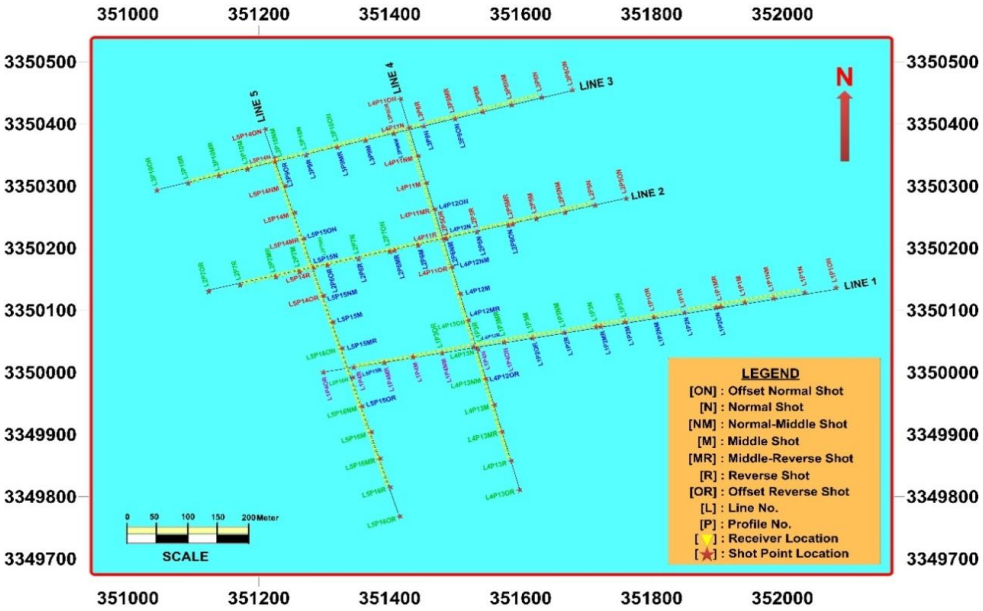

Figure (7): Shot point location map.

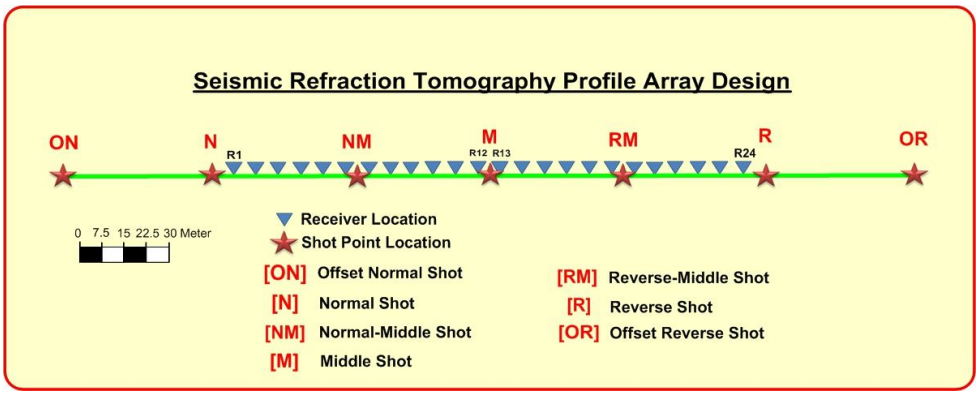

Figure (8): Seismic Refraction Tomography array design.

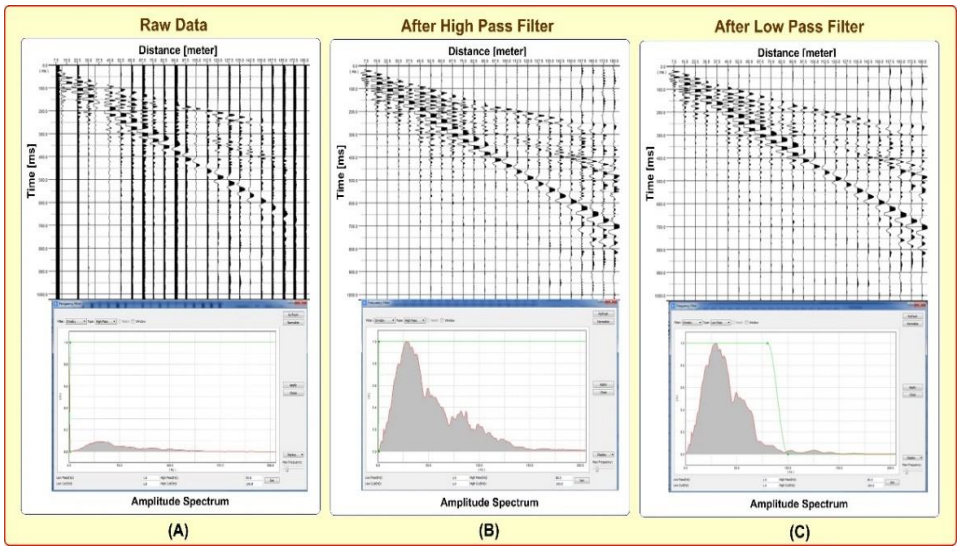

Figure (9): Filtering processes steps applied on the raw seismic data (A), (B) seismic data after High-Pass Filter and (C) seismic data after Low-Pass Filter.

Figure (9) shows an example of a shot record from the acquired data (Line 2 – spread1 – Normal Shot), where (A) represents the raw data shot record with its corresponding amplitude spectrum, (B) represents the shot record after applying the high-pass filter with its corresponding amplitude spectrum and (C) represents the shot record after applying the low-pass filter with its corresponding amplitude spectrum.

Filtered refraction data (shot records) were analyzed using the software program Zond2DST, *Zond Geophysical Software*. First arrival times were picked, as shown in Figure (10)and the travel time curves are constructed, based on the distance along the survey line, geophone intervals, source location, and the first arrival times.

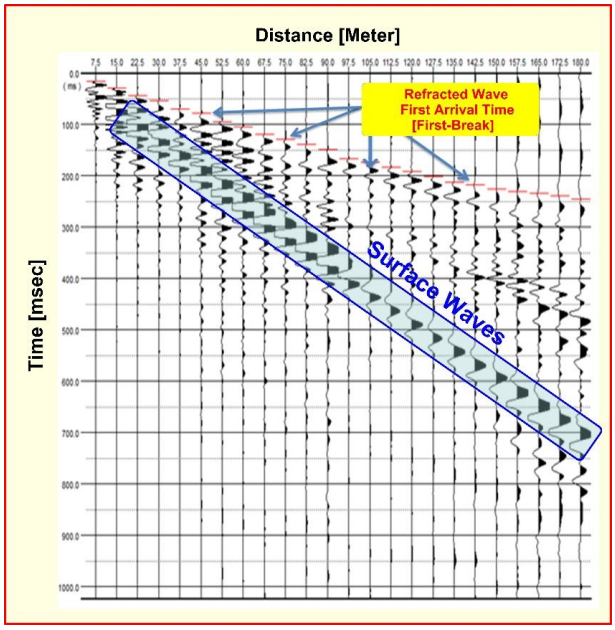

Figure (10): Picking of the first arrival times, line 2 – Profile 1 – Normal Shot.

The travel time curves are corrected and checked for the exact estimation of the compressional (V_p) wave velocity. The observed travel times are inverted into velocity models using the smoothing and layered inversion methods, depending on the initial model from the previous geological and geophysical information of the study area. The best fitting between the observed (measured) and calculated (after inversion process) travel times has root mean square (RMS) error 3.15, 3.60, 3.61, 3.45 and 3.00 % for line 1, line 2, line 3, line 4 and line 5, respectively. The lowest RMS error value indicates a best fit between the observed and calculated travel times.

The surface waves seismic data are processed using the software program Zond2DST, Zond Geophysical Software, through spectral inversion to obtain 1D and 2D MASW shear wave velocity profiles. Common mid-point (CMP) pairs from all the traces were extracted and then their cross correlation CMP gathers were calculated. Thereafter, the dispersion curves are generated by converting them into frequency domains for each cross correlation CMP gathers and then checked. The dispersion curves are generally displayed as phase velocity versus frequency, as shown in Figure (11).

The generated dispersion curves for each shot record are inverted into 1D shear wave velocity model. Then, all the shot records along the seismic line were inverted to generate the 2D shear wave velocity model for each seismic line. Figure (12) shows an example of the 2D inversion of the shear wave velocity model for line 2.

Figures (13A), (14A), (15A), (16A) and (17A) represent the inverted compressional wave (V_p) velocity models for line 1, line 2, line 3, line 4 and line 5, respectively. While, Figures (13B), (14B), (12B), (15B),(16B) and(17B) represent the inverted shear wave (Vs) velocity models for line 1, line 2, line 3, line 4 and line 5, respectively.

The elastic properties of rocks can be described by elastic constants; such as Young's modulus (E), Bulk modulus (K), Rigidity or shear modulus (μ) and Poisson's ratio (σ).These elastic constants are ratios of stress to strain with the different constants defined in terms of different stresses; such as tension, compression and shear, and the deformation or strain produced.

Geotechnical Parameters and Dynamic Characteristics

As long as the compressional wave velocity V_p and shear wave velocity V_s obtained, all the elastic moduli and geotechnical parameters can be calculated. The first step in the elastic moduli and geotechnical parameters calculation flow chart is the calculation of the density (ρ).

1. Density (ρ):

According to Nafe and Drake (1963) and Gardner et al. (1974)the density can be calculated through the following equation (1):

$$\rho = a\, V_p^{\frac{1}{4}} \quad (1)$$

where: (a) is a constant equals 0.31, when the density is given in g/cm^3 and V_p is in m/s.

2. Poisson's ratio (σ):

The Poisson's ratio is the ratio of the change in shape of a body due to the applied force. If a compressive force is applied to a body, a decrease in the length of the body will occur in the direction parallel to the force and an increase in width will occur perpendicular to the force. If the applied force is tension, the opposite change in dimensions will occur. According to Telford et al., (2003), the Poisson's ratio can be calculated through equation (2).

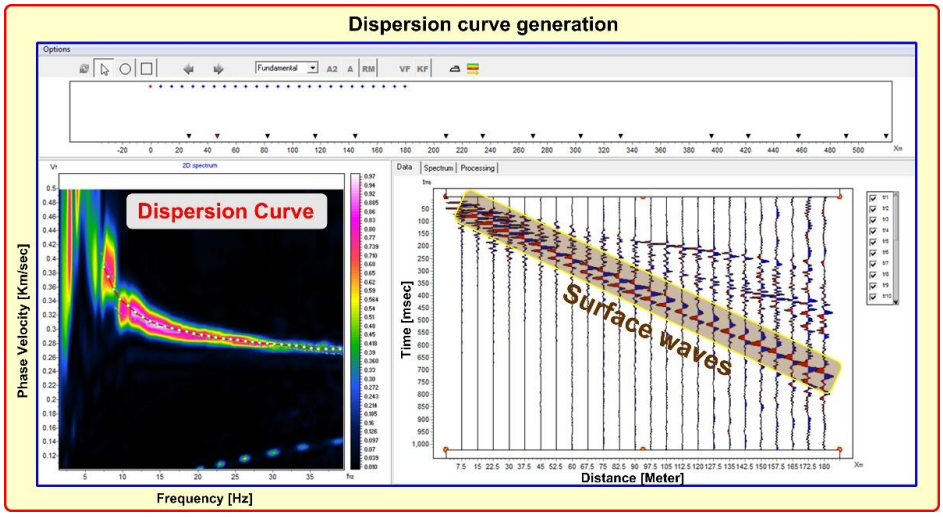

Figure (11): Dispersion curve generation.

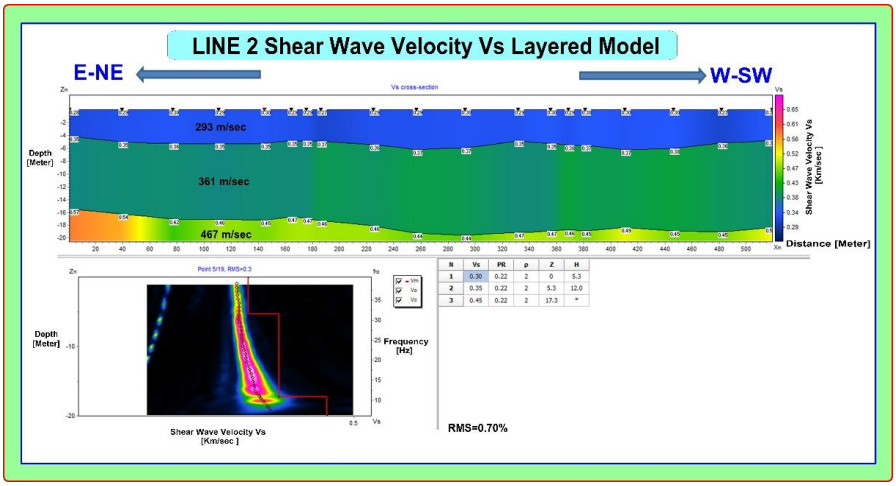

Figure (12): 2D Inversion of shear wave velocity model for line 2.

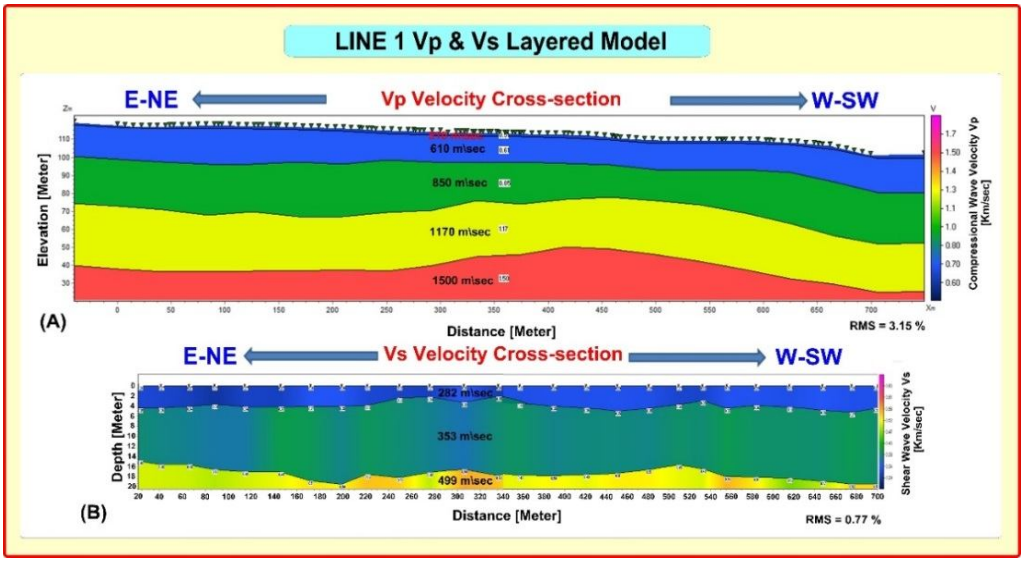

Figure (13): Line 1 velocity models where (A), Compressional wave (V_p) velocity model and (B), Shear wave (V_s) velocity model.

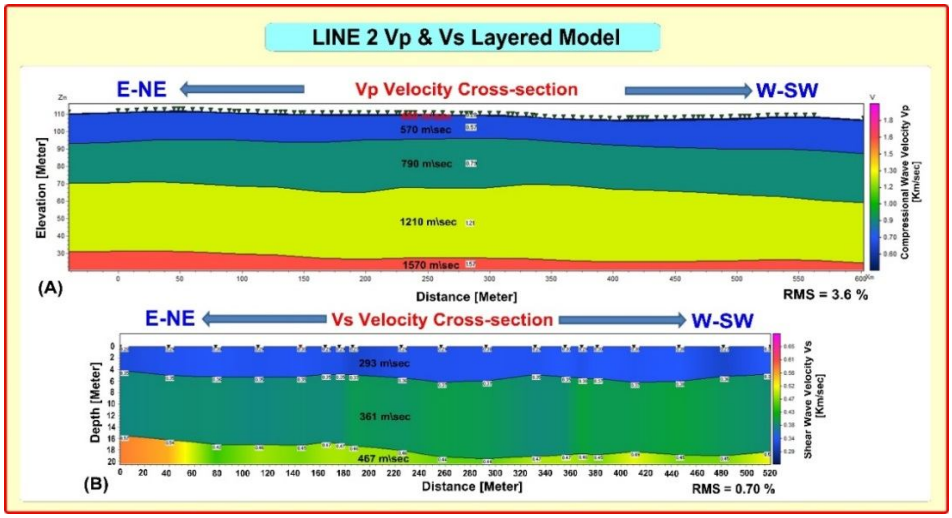

Figure (14): Line 2 velocity models where (A), Compressional wave (V_p) velocity model and (B), Shear wave (V_s) velocity model.

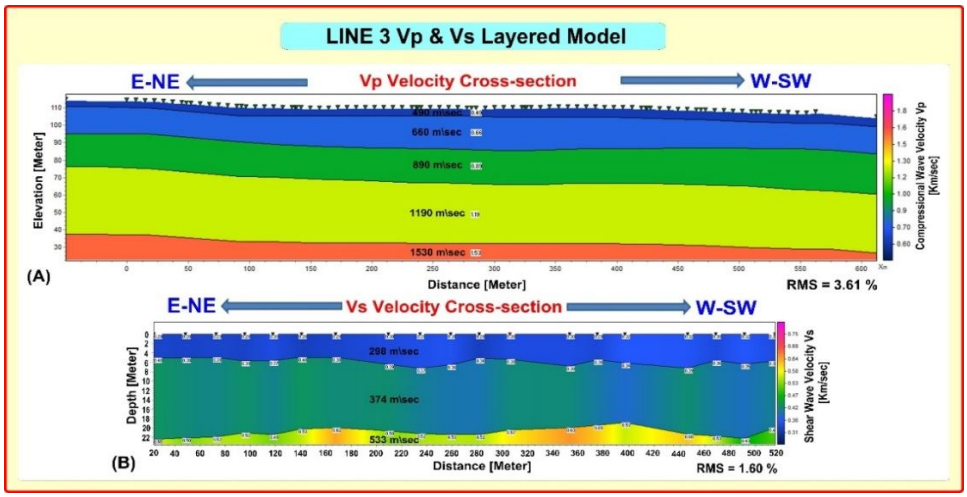

Figure (15): Line 3 velocity models where (A), Compressional wave (V_p) velocity model and (B), Shear wave (V_s) velocity model.

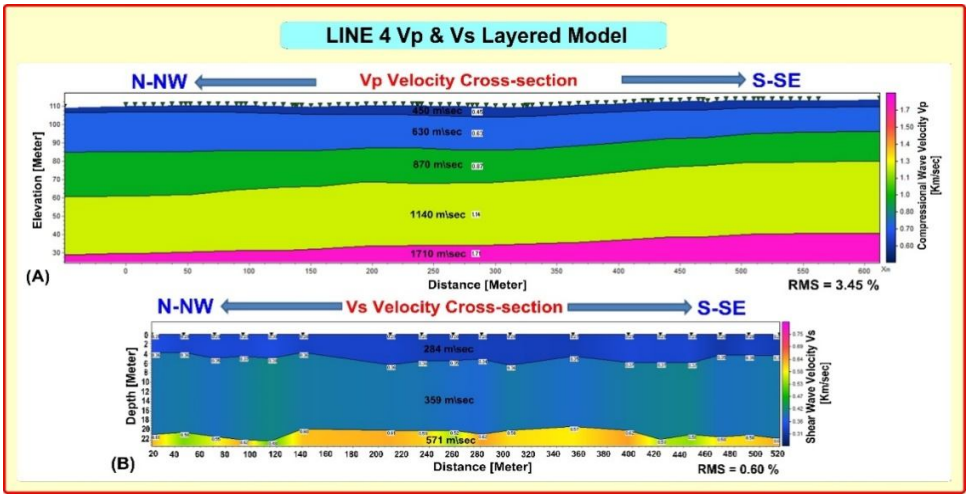

Figure (16): Line 4 velocity models where (A), Compressional wave (V_p) velocity model and (B), Shear wave (V_s) velocity model.

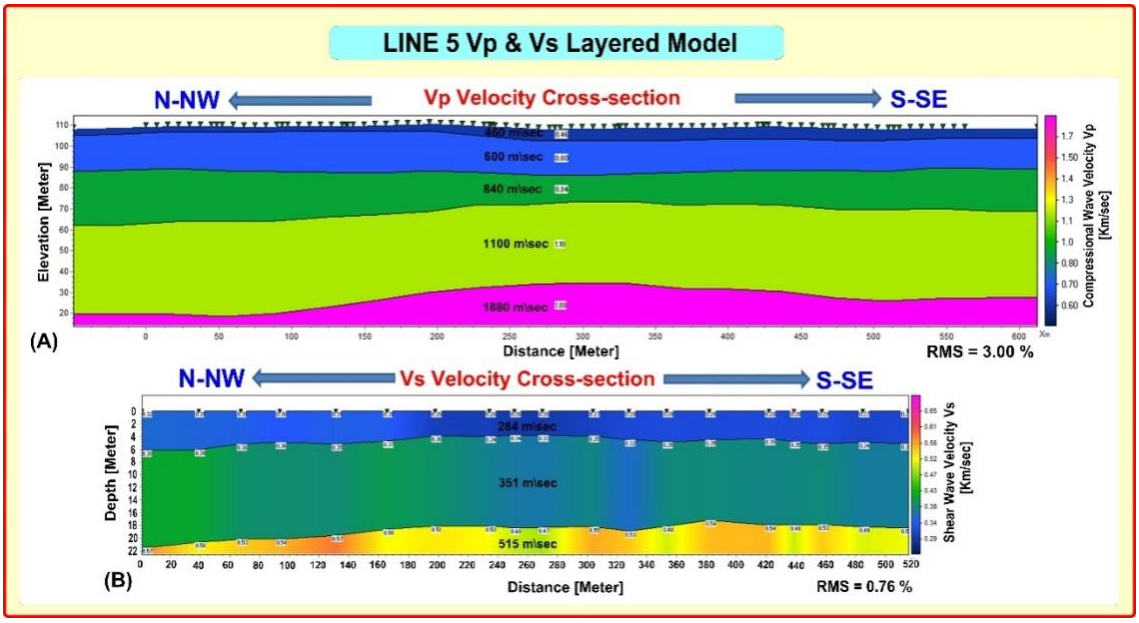

Figure (17): Line 5 velocity models where (A), Compressional wave (V_p) velocity model and (B), Shear wave (V_s) velocity model.

$$\sigma = \frac{((V_P/V_S)^2-2)}{(2(V_P/V_S)^2-2)} \quad (2)$$

3. Rigidity modulus (μ):

The rigidity or shear modulus is the stress-strain ratio for direct shear. It is determined as the shearing stress (F/A), which is the force tangential to the surface displaced per shearing strain (ΔL/L),that is the displacement (ΔL) in the line of force per unit length (L) perpendicular to the line of force. It also has units of force per unit area, commonly *psi* (pounds per square inch). According to Sharma (1978), the rigidity modulus can be calculated through equation (3).

$$\mu = \rho V_S^2 \quad (3)$$

4. Young's modulus (E)

The Young's modulus is the stress-strain ratio in simple tension or compression. The force or stress applied per unit area divided by the unit shortening or lengthening defines the Young's modulus (Nettleton, 1940), where E has the units of force per unit area, commonly pounds per square inch (psi). According to Lowrie (1997), the young's modulus can be calculated through equation (4).

$$E = 2(1+2\sigma)\mu \quad (4)$$

5. Bulk modulus (K)

The Bulk modulus is the stress-strain ratio under uniform compressive stress in all directions. The stress is force per unit area and the strain is the proportional change in volume. According to Abd El-Rahman (1989) and Mott et al. (2008), the bulk modulus can be calculated through equation (5).

$$K = \frac{E}{3(1-2\sigma)} \quad (5)$$

Using the seismic wave velocities (V_p and V_s) andthe elastic moduli values, the shallow soil engineering parameters are calculated, these parameters include the Material index(M_i), Concentration Index (C_i) and the Stress Ratio(S_i). The full description and values ranges of these parameters are well explained by Adams, (1951), Brich, (1966), Gassman, (1973), Bowless, (1982), Sheriff and Geldart, (1986),Abd El-Rahman, (1989) andAbd El-Rahman, (1991).

6. Material index(M_i):

According to Abd El-Rahman (1989),the Material index (M_i) can be calculated through equation (6).

$$M_i = (1-4\sigma) \quad (6)$$

7. Concentration Index (C_i):

According to Abd El-Rahman (1989), the Concentration Index (C_i)can be calculated through equation (7).

$$(C_i) = (3-4\alpha)/(1-2\alpha) \quad (7)$$

where: α is the velocity squared ratio, $\alpha = (V_S^2 / V_P^2)$.

Table 1: Site classification scheme of NEHRP provisions (2003).

Site Class	Site Description	Parameters	
		V_S(30) [m/sec]	N_{SPT}
A	Hard rock	>1500	--
B	Rock	760–1500	--
C	Very dense soil and soft rock	360–760	>50
D	Stiff soils	180–360	15–50
E	Soft soils, profile with more than 10 ft (3 m) of soft clay	180	<15
F	Soils requiring site specific evaluations	--	--

Table 2: Geotechnical Parameters and Dynamic Characteristics of layer 1.

Parameter	Layer 1					
	Line 1	Line 2	Line 3	Line 4	Line 5	Average
Thickness [meter]	4.18	5.34	5.43	4.94	4.77	4.93
Vp [m/sec]	510	480	490	450	460	478.00
Vs [m/sec]	282	293	298	284	284	288.20
Site Class	D	D	D	D	D	D
Density (ρ) [g/cm^3]	1.47	1.45	1.46	1.43	1.44	1.45
Poisson's Ratio (σ)	0.28	0.20	0.21	0.17	0.19	0.21
Rigidity or Shear Modulus (μ) [Dyn/cm2]	1.17E+09	1.25E+09	1.30E+09	1.15E+09	1.16E+09	1.20E+09
Young's Modulus (E) [Dyn/cm^2]	3.65E+09	3.50E+09	3.66E+09	3.08E+09	3.21E+09	3.42E+09
Bulk Modulus (K) [Dyn/cm^2]	2.77E+09	1.97E+09	2.08E+09	1.55E+09	1.73E+09	2.02E+09
Material Index (Mi)	-0.12	0.19	0.17	0.32	0.23	0.16
Velocity Squared Ratio	0.31	0.37	0.37	0.40	0.38	0.37
Concentration Index (Ci)	4.57	5.92	5.84	6.92	6.21	5.89
Stress Ratio (Si)	0.39	0.25	0.26	0.20	0.24	0.27
Ultimate bearing capacity (Qult) [Kg/cm^2]	0.86	0.96	1.01	0.87	0.87	0.91

Table 3: Geotechnical Parameters and Dynamic Characteristics of layer 2.

Parameter	**Layer 2**					
	Line 1	**Line 2**	**Line 3**	**Line 4**	**Line 5**	**Average**
Thickness [meter]	11.95	12.59	12.67	13.95	14.03	13.04
Vp [m/sec]	610	570	660	630	600	614.00
Vs [m/sec]	353	361	374	359	351	359.60
Site Class	D	C	C	D	D	D
Density (ρ) [g/cm^3]	1.54	1.51	1.57	1.55	1.53	1.54
Poisson's Ratio (σ)	0.25	0.17	0.26	0.26	0.24	0.24
Rigidity or Shear Modulus (μ) [Dyn/cm^2]	1.92E+09	1.97E+09	2.20E+09	2.00E+09	1.89E+09	2.00E+09
Young's Modulus (E) [Dyn/cm^2]	5.75E+09	5.25E+09	6.71E+09	6.08E+09	5.59E+09	5.88E+09
Bulk Modulus (K) [Dyn/cm^2]	3.80E+09	2.61E+09	4.73E+09	4.22E+09	3.58E+09	3.79E+09
Material Index (Mi)	0.01	0.34	-0.05	-0.04	0.04	0.06
Velocity Squared Ratio	0.33	0.40	0.32	0.32	0.34	0.34
Concentration Index (Ci)	5.03	7.06	4.80	4.85	5.17	5.38
Stress Ratio (Si)	0.33	0.20	0.36	0.35	0.32	0.31
Ultimate bearing capacity (Qult) [Kg/cm^2]	1.65	1.77	1.96	1.74	1.63	1.75

Table 4: Geotechnical Parameters and Dynamic Characteristics of layer 3.

Parameter	**Layer 3**					
	Line 1	**Line 2**	**Line 3**	**Line 4**	**Line 5**	**Average**
Thickness [meter]	24.47	23.53	19.62	21.63	21.87	22.22
Vp [m/sec]	850	790	890	870	840	848.00
Vs [m/sec]	499	467	533	571	515	517.00
Site Class	C	C	C	C	C	C
Density (ρ) [g/cm^3]	1.67	1.64	1.69	1.68	1.67	1.67
Poisson's Ratio (σ)	0.24	0.23	0.22	0.12	0.20	0.20
Rigidity or Shear Modulus (μ) [Dyn/cm^2]	4.17E+09	3.58E+09	4.81E+09	5.49E+09	4.43E+09	4.50E+09
Young's Modulus (E) [Dyn/cm^2]	1.23E+10	1.05E+10	1.39E+10	1.36E+10	1.24E+10	1.25E+10
Bulk Modulus (λ) [Dyn/cm^2]	7.79E+09	6.51E+09	8.26E+09	6.01E+09	6.85E+09	7.08E+09
Material Index (Mi)	0.05	0.07	0.12	0.51	0.20	0.19
Velocity Squared Ratio	0.34	0.35	0.36	0.43	0.38	0.37
Concentration Index (Ci)	5.22	5.32	5.54	9.22	6.03	6.27
Stress Ratio (Si)	0.31	0.30	0.28	0.14	0.25	0.26
Ultimate bearing capacity (Qult) [Kg/cm^2]	4.56	3.76	5.54	6.78	5.01	5.13

8. Stress Ratio (S_i):

According to Thomson (1986), the Stress Ratio (S_i) can be calculated through equation (8).

$$(S_i) = 1 - 2(V_S^2 / V_P^2) \quad (8)$$

9. Ultimate-bearing capacity (Q_{ult}):

The ultimate-bearing capacity (Q_{ult}) can be defined as "the maximum load required for shear failure or sand liquefaction". This capacity is controlled by the shear strength factor. According to Bowles (1984) and Abd El-Rahman et al. (1992), the ultimate-bearing capacity (Q_{ult}) can be calculated through equation (9)

$$\log Q_{ult} = 2.932\,(\log Vs - 1.45) \quad (9)$$

10. Site classification:

The sites are classified in accordance with the NEHRP Provisions (BSSC, 2003) and Eurocode 8 (CEN, 2003) (Table 1), both of which suggest the criteria based on the mean shear wave velocity $V_S(30)$ and the mean penetration resistance (N_{SPT}) of the uppermost 30 m of soil/rock profile.

RESULTS

The soil section presented in the area of study consists of three layers, based on the compressional wave (V_P) and shear wave (V_S) velocities models. The top layer (Layer 1) belongs to the Quaternary surficial deposits composed of loose sand and gravel, it has an average compressional wave velocity of(478 m/sec) and an average shear wave velocity of(288.20 m/sec) across the five seismic lines. It is underlained by the second layer (Layer 2),which belongs to the Middle Miocene age *Hommath Formation*. It is composed of low to medium dense sand, with an average compressional velocity of (614 m/sec) and an average shear wave velocity of (359.6 m/sec) across the five seismic lines. The second layeroverlies the third layer (Layer 3), which belongs to the Middle Miocene age *Hommath Formation*. It is composed of medium to high dense sand, with an average compressional wave velocity of (848 m/sec) and an average shear wave velocity of (517 m/sec)across the five seismic lines.

Based on the values of compressional and shear wave velocities of the generated velocity models for each seismic line, the geotechnical parameters and the dynamic characteristics of the soil layers presented in the study area can be calculated. Tables (2), (3) and (4) represented the calculated geotechnical parameters and the dynamic characteristics for layer 1, layer 2 and layer 3, respectively. According to the **Site Classification Scheme of NEHRP Provisions (2003),** the presented soil layer 1, layer 2 and layer 3 are classified into (D, D and C classes),respectively.

Based on the values of the compressional wave (V_P) and shear wave (V_S) velocity models; we tried to deduce an equation representing the relationship between (V_P) and (V_S) for the soil layers in the study area. This was done by sketching the values of (V_P) and (V_S) at the same positions through the seismic lines acquired. Figure (18) shows the relationship between the velocity types; where the X-axis represents the compressional wave velocity (V_P) and the Y-axis illustrates the shear wave velocity (V_S). By drawing the best fit line for the data points; it is found that, the relationship is almost linear represented by the shown straight line equation, where (V_S) is directly proportional to the (V_P) multiplied by a constant of (0.6014). Equation (9) shows the relationship between (V_S) and (V_P).

$$V_S = 0.6014\,V_P \quad (9)$$

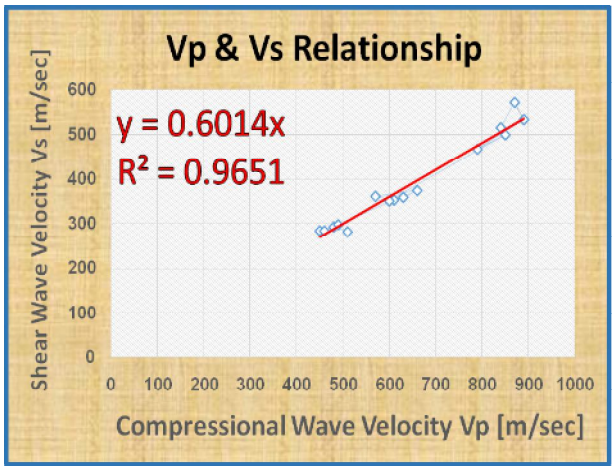

Figure (18): Relationship between the compressional wave velocity (V_p) and shear wave velocity (V_s) for the soil layers present in the study area.

SUMMARY AND CONCLUSIONS

The use of shallow seismic refraction tomography and MASW techniques for the determination of the geotechnical parameters and engineering site characteristics has received considerable attention over the last number of years. MASW is a recently developed seismic method, that deals with the relatively lower frequencies and shallower investigation depth ranges than do the conventional high-resolution seismic methods. It provides shear-wave velocity (V_S) information of the near-surface materials. Although

seismic refraction tomography is a geophysical method for interpreting the seismic refraction data, which uses a gridded, inversion technique to determine the velocities of individual 2-dimensional blocks (pixels) within a profile, as opposed to model the velocities as layers. It provides compressional wave velocity (V_P) information, with better resolution of the complex velocity structure of the subsurface geologic structures.

Sixteen seismic refraction tomography profiles along five seismic lines have been acquired in the study area. Seismic refraction tomography and MASW techniques were used to generate preliminary depth velocity models. The generated compressional wave (V_P) and shear wave (V_s) velocity models showed that, the soil presented in the study area can be differentiated into three layers according to the change in the velocities, as follow:

1) **Layer 1:** The top layer has an average compressional wave velocity of about 478 m/sec, and an average shear wave velocity of about 288.2 m/sec,with an average thickness of about 4.93 m, where it is composed of sand and gravel belonging to the Quaternary surficial deposits. Based on the values of V_p and V_s,this layer has an average density of about1.45g/ cm^3 , Poisson's Ratio≈ 0.21, Young's Modulus≈3.42E+09 Dyn/ cm^2, Rigidity Modulus≈1.20E+09 Dyn/cm^2, Bulk Modulus≈2.02E+09 Dyn/cm^2, Material Index≈0.16, Concentration Index≈5.89, Stress Ratio≈ 0.27 and Ultimate Bearing Capacity ≈0.91 Kg/cm^2.

2) **Layer 2:**The second layer, which underlies the Quaternary surficial deposits, has compressional wave velocity of about 614 m/sec, and shear wave velocity of about 339.60m/sec, with an average thickness of about 13.04 m. It is composed of sand, that belongs to the Middle Miocene *Hommath Formation*. Based on the values of V_p and V_s, it has an average density ≈ 1.54 g/cm^3, Poisson's Ratio≈ 0.24, Young's Modulus ≈5.88E+09Dyn/cm^2, Rigidity Modulus ≈ 2.00E+09 Dyn/cm^2, Bulk Modulus ≈ 3.79E+09 Dyn/cm^2, Material Index≈0.06, Concentration Index≈5.38, Stress Ratio≈ 0.31 and Ultimate Bearing Capacity≈ 1.75 Kg/cm^2.

Layer 3: The third layer, which underlies layer 2, has compressional wave velocity of about 848 m/sec, and shear wave velocity of about 517 m/sec, with an average thickness of (22.22 m). It is composed of sand, that belongs to the Middle Miocene *Hommath Formation*. Based on the values of V_p and V_s,it has an average density of about 1.67g/cm^3, Poisson's Ratio ≈ 0.20, Young's Modulus ≈1.25E+10 Dyn/cm^2, Rigidity Modulus ≈4.50E+09 Dyn/cm^2, Bulk Modulus ≈ 7.08E+09 Dyn/cm^2, Material Index ≈ 0.19, Concentration Index ≈6.27, Stress Ratio ≈ 0.26 and Ultimate Bearing Capacity ≈ 5.13 Kg/cm^2).

The integration and combination between the seismic refraction tomography and MASW technique give reliable information about the compressional wave and shear wave velocities and characteristics of the interfaces within the near-surface layers in the study area.

The near-surface soil layers presented in the study area are classified into two site classes, (D and C) according to the Site Classification Scheme of NEHRP Provisions (2003).

The relationship between the compressional wave velocity and the shear wave velocity for the near-surface layers, presented in the study area, can be identified by a linear equation ($V_S = 0.6014\, V_P$).

REFERENCES

Abd El-Rahman, M., (1989): Evaluation of the kinetic moduli of the surface materials and application to engineering geologic maps at Ma'Barrisabah area (Dhamar province). North. Yemen. Egypt. J. Geol. 33 (1–2), p. 229–250.

Abd El-Rahman, M., Setto, I., and El-Werr, A., (1992): Inferring mechanical properties of the foundation materials at the 2nd Industrial zone city, from geophysical measurements E.G.S. Proc. of the 10th Ann. Meet, p. 50–61.

Abd El-Rahman, M., (1991): The potential of coefficient and seismic quality factor in delineating less sound foundation materials in JabalShibAz Sahara area, Northwest of Sanaa, Yemen Arab Republic, Egypt, M. E. R. C. Earth Sci., vol. 5. Ain Shams University, p. 181-197.

Adams, L.H., (1951): Elastic properties of materials of the earth crust, internal construction of the earth (edited by Gutenberg), Dover publications, Inc., New York.

Araffa, S.A.S., Helaly, S.A., Khozium, A., Lala, S.M. S., Soliman, A.S., Hassan, M.N., 2015: Delineating groundwater and subsurface structures by using 2D resistivity, gravity and 3D magnetic data interpretation around Cairo–Belbies Desert road, Egypt, NRIAG Journal of Astronomy and Geophysics (2015) 4, p. 134–146.

Bowles, J.E., (1984): Physical and Geotechnical Properties of Soils. Mc Grew- Hill, London.

Brich, F., (1966): Handbook of physical constants, Geol. Soc. Amer. Men. 97, pp 613**.**

Bowles, J.E., (1982): Foundation analysis and design, 2nd Ed. McGraw-Hill International Boo; Company, London, pp 587.

El-Hadidy, M.S., (2012): Seismotectonics and seismic hazard studies in and around Egypt. PhD thesis, Faculty of Science, Ain Shams University, Egypt.

Gardner, G. H. F., Gardner, L. W., and Gregory, A. R., (1974): Formation velocity and density; the diagnostic basics for stratigraphic traps, Geophysics, 39, p. 770–780.

Gassman, F., (1973): Seismischeprospektion, Birkhacuserverlag, Stuttagart, pp 417.

Gretener, P., (2003): Summary of the Poisson's Ratio Debate 1990–2003, Feature Article, CSEG recorder, September 2003, p. 44–45.

Geological Survey of Egypt (EGSMA), (1998): Geology of Inshas Area, Geol. Surv. Of Egypt, internal report.

Kesarwani, A., Sharma, A., Jain, C., (2012): MASW versus Refraction Seismic Method in terms of acquisition and processing of data and the accuracy of estimation of velocity profiles, 9th Biennial International Conference & Exposition on Petroleum Geophysics, p. 320-324.

Lowrie, W., (1997): Fundamentals of Geophysics. Cambridge University Press, p. 354.

Mott, P.H., Dorgan1, J.R., Roland, C.M., (2008): The bulk modulus and Poisson's ratio of ''incompressible'' materials. J. Sound Vibrat. 312, p. 572–575.

Nafe, J.E., Darke, C.L., (1963): Physics properties of marine sediments. In: Hill, M.N. (Ed.), In: The Sea, vol. 3. Interscience Publishers, New York, p. 794–815.

NEHRP, (2003): Recommended provisions for seismic regulations for New Buildings and Other Structures. Building Seismic Safety Council (BSSC) for the Federal Emergency Management Agency (FEMA 450). Washington, Part 1: Provisions.

Riad, S., Ghalib, M., El-Difrawy, M.A., Gamal, M., (2000): Probabilistic seismic hazard assessment in Egypt. Ann. Geol. Surv. Egypt. XXIII: pp 851.

Sharma, P.V., (1978): Geophysical Methods in Geology, Seconded. Elsevier, Oxford, New York.

Sheriff, R.E., Geldart, L.P., (1986): Exploration Seismology, Cambridge Univ, Press, Cambridge, pp 316.

Richart, F.E., Hall, J.R. and Woods, R.D., (1970): Vibrations of Soils and Foundations. Prentice-Hall, Englewood Cliffs, New Jersey, U.S.A., pp 414.

Tokeshi, K., Harutoonian, P., Leo, C.J., Liyanapathirana, S., (2013): Use of surface waves for geotechnical engineering applications in Western Sydney, Adv. Geosci., 35, p. 37–44.

Thomson, L., (1986): Weak elastic anisotropy, Geophys. Prospect, 51, p. 1954–1966**.**

Park, C.B., Miller, R.D., and Xia, J., (1997): Multi-channel analysis of surface waves (MASW) "A summary report of technical aspects, experimental results, and perspective", Kansas Geological Survey,

Park, C. B., Miller, R. D., and Xia, J., (1998): Imaging dispersion curves of surface waves on multi-channel record, Expanded Abstracts of 68th Ann Mtng of Society of Exploration Geophysicists, Louisiana, p. 1377-1380.

Park, C.B., Miller, R.D., & Xia, J. (1999): Multi-channel analysis of surface waves. Geophysics 64, No. 3, p. 800-808.

Park, C.B., Miller, R.D., Ryden, N., Xia, J., and Ivanov, J., (2005): Combined use of active and passive surface waves: Journal of Engineering and Environmental Geophysics (JEEG), 10, (3), p. 323-334.

Xia, J., Miller, R.D. and Park, C.B. (1999): Estimation of near surface shear-wave velocity by inversion of Rayleigh waves, Geophysics, 64, p. 691–700.

Yordkayhun, S., Sujitapan, C., Chalermyanont, T., (2014): Joint analysis of shear wave velocity from SH-wave refraction and MASW techniques for SPT-N estimation, Songklanakarin J. Sci. Technol, 36 (3), p. 333-344.